Low Temperature Physics/Fizika Nizkikh Temperatur, 2017, v. 43, No. 8, pp. 1131–1136

Inhomogeneous broadening of the conductance histograms for molecular junctions

Julian M. Bopp, Sumit Tewari, Carlos Sabater, and Jan M. van Ruitenbeek

Kamerlingh Onnes Laboratorium, Universiteit Leiden, Postbus 9504, 2300 RA Leiden, The Netherlands
E-mail: ruitenbeek@physics.leidenuniv.nl

Received January 25, 2017, published online June 26, 2017

We demonstrate that the notched-wire mechanically controllable break junction technique can be exploited for the study of single molecule junctions. We have developed a protocol for deposition of thiol-coupled molecules onto Au electrodes from solution. We find surprisingly sharp conductance historgrams at low temperatures, which suggest that the commonly observed large width of the peaks in conductance historgams is the result of inhomogeneous broadening.

PACS: **73.22.–f** Electronic structure of nanoscale materials and related systems;
73.63.–b Electronic transport in nanoscale materials and structures;
73.63.Rt Nanoscale contacts;
Keywords: break junctions, MCBJ, molecular electronics, OPE3, conductance histogram.

1. Introduction

Electron transport across individual molecules has long been recognized as a very interesting field of study in terms of the theoretical concepts involved, and from an applications perspective. Since a little more than a decade techniques have been developed in various labs around the world that have established single-molecule junctions as a platform for experimental study. The techniques mostly rely on some form of metal-electrode breaking, such that a gap is formed of the proper size for bridging by a single molecule. The most widely employed methods are mechanically controllable break junctions [1–3] (MCBJ), modified scanning tunneling microscopes [4–10] (STM) or atomic force microscopes [11,12] (AFM), and bridges formed by electromigration of a nanofabricated metal wire [13,14].

When studies at cryogenic temperatures are required, as is needed to obtain sufficient resolution for resolving the electronic and vibrational structure of a molecule from differential conductance or shot noise measurements, STM and AFM techniques become very elaborate. The drawbacks of these methods are that in-situ ultra-high-vacuum preparation of samples and tips and vacuum deposition of molecules impose constraints on the types of molecules, the experiments are very time-consuming, and the system is usually not well adapted for shot noise measurements. A large part of the progress in the field has come from the other, much simpler approaches. Break junction techniques have been widely explored, which have the great advantage that massive statistics of junction properties can be obtained in a reasonable time by repeated making and breaking of molecular contacts.

At this point we need to distinguish two kinds of MCBJ techniques: Lithographic break junctions (L-MCBJ) and notched wire break junctions (NW-MCBJ), each having its own specific advantages and disadvantages [15]. L-MCBJ (Fig. 1(a)) have been most widely exploited for the study of molecular junctions, and these are fabricated by means of electron-beam lithography (for details, see Ref. 2). A bridge of about 2 μm long having a constriction of about 100 nm wide is carved into a metal film, and this metal is usually taken to be Au. The metal film rests on an insulating layer (e.g., polyimide) that is deposited onto a flexible substrate such as phosphorous bronze or stainless steel. By isotropic ion etching of the insulating layer the bridge becomes freely suspended. By mounting this structure into a three-point bending configuration the top of the substrate that holds the nanobridge can be controllably stretched up to the point of breaking of the bridge in the metal film. By relaxing the bending the contact in the bridge can be re-establised. Molecules are usually deposited from solution at room temperature, either before the intial breaking or thereafter. The molecules typically have chemical anchor groups at two ends that are designed to bind to the metal surfaces of the bridge. Most commonly thiols are used for anchoring to Au.

The NW-MCBJ technique was developed first, and is simpler in that it does not require time-consuming clean-room procedures [1,16]. It starts from a regular metal wire

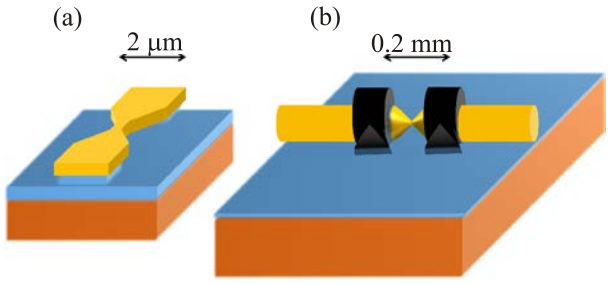

Fig. 1. Illustration of the lithographic MCBJ technique (a), and the notched-wire MCBJ technique (b).

of about 0.1 mm in diameter, with a constriction formed manually by means of a sharp knife. Glueing this wire onto a similar bendable substrate results in a junction that can be broken and controlled by bending of the substrate, similar to the L-MCBJ technique described above.

The NW-MCBJ technique has been exploited widely for the study of metallic atomic contacts, because the method can be easily applied to nearly any metal in the periodic system. Metal deposition and grain growth properties limit L-MCBJ to a small subset of metallic elements. On the other hand, the much smaller bridge length of the L-MCBJ leads to a greatly enhanced mechanical stability, which is why it has become the method of choice for study of molecular junctions at low temperatures.

Apart from the more elaborate fabrication method of L-MCBJ compared to NW-MCBJ, one of the main drawbacks is the limitation in obtaining junction statistics. The L-MCBJ has a very small displacement ratio, which is the ratio between the increase in distance between the two broken bridge ends and the displacement of the piston pushing in the middle of the back of the substrate. The displacement ratio is determined by the dimensions of the bridge and is typically smaller than 10^{-5}. While this is favorable for a high mechanical bridge stability it seriously limits the range of distances for the bridge ends when using a piezo-electric element for control of the bending. Typically, piezo-elements at low temperatures can produce length changes of the order of 1 μm, which translates by the displacement ratio into a change of bridge distance of only 0.01 nm. This can be solved by using an electromechanical drive, but this limits the speed of operation by at least two orders of magnitude. Since characterization of molecular junctions is usually done by taking thousands of contact making and braking cycles, this initial step in the experiments can take up to a day for L-MCBJ. The displacement ratio for NW-MCBJ is only about $3{\cdot}10^{-3}$, allowing fast piezo-electric control of the bending cycles, which permits reducing this initial step to only 10 minutes.

Methods for introducing molecules to the junctions should meet requirements of suitable dosage and should avoid contamination of the contact surfaces by foreign molecules. For small molcules it has been demonstrated that molecules can be deposited from a vapour source at room temperature through a capillary leading to the junction at low temperatures [17–21]. For a wide class of interesting organic molecules this method is impractical and the most frequently taken approach is to deposit molecules from solution at room temperature before cooling down the break junction device [15,22,23]. The risk of contamination is mitigated by selecting gold electrodes, which have a small tendency to bind to many common contaminants, and thiol anchoring groups on the molecules, which strongly bind to gold. Usually the deposition is done quickly and under a controlled inert atmosphere of nitrogen or argon gas in order to further limit the risk of contamination. For L-MCBJ devices the molecules can be deposited before the intial breaking of the junction, but usually repeated breaking at room temperature is used for verifying the presence of molecules in the junction from the conductance traces.

Methods for introducing molecules from solution are well established for L-MCBJ, but have hardly been tested for NW-MCBJ. The larger size of the metal wires may limit the diffusion of the molecules to the active junction area, and the different materials used in the fabrication may lead to contamination. For this reason it is useful that we, here, demonstrate that the NW-MCBJ technique can be employed at low temperatures for studying thiol-coupled molecules deposited from solution. We find that the molecular junctions are surprisingly stable. Moreover, we observe that the peaks obtained in the histograms switch spontaneously between positions as a function of time, which we attribute to the switching of the dominant molecular binding configurations that are probed during the breaking cycles.

2. Experimental techniques

A phosphorous bronze sheet, 0.8 mm thick and approximately 3 cm long and 5 mm wide, forms the bendable substrate of a NW-MCBJ device. A layer of thin kapton foil is glued on top of this substrate in order to insulate the substrate electrically from the electrode wires. The wire that will be broken to form the electrodes to the molecules is 99.99% pure gold with a diameter of 0.1 mm. A surgical knife blade in a height-adjustable mount is used for cutting a sharp notch in the center of the wire. Slow-hardening Stycast epoxy glue is deposited on either side of the notch and gradually pressed closer to the notch. Electrical contacts on both sides are connected by silver epoxy.

The conductance of the junction is measured in a two-probe configuration by applying a bias voltage through a National Instruments data acquisition card connected to a desktop PC. For the present experiments we have used bias voltages in the range from 40 to 80 mV. The current is measured by a Stanford Research Systems low-noise linear current amplifier SR570. The current levels are read by the same PC through a GPIB link. The piezo actuator is con-

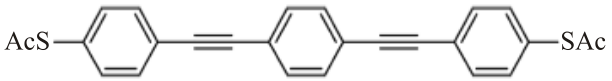

Fig. 2. Chemical structure of the OPE3 molecules used in this study.

trolled by a high voltage source which amplifies a control voltage also delivered from the data acquisition card. The measurements are controlled and the data are stored and analysed by a Labview-based routine.

For the purpose of this work we have selected the much studied molecule OPE3, which is the three-monomers version of oligo(phenylene ethynylene), having acetyl-protected thiol groups at both ends, (see Fig. 2). OPE3 is a conjugated rod-like molecule with a conductance of $1–2\cdot10^{-4}G_0$ [24–26], where $G_0 = 2e^2/h$ is the conductance quantum. For the deprotection of the anchor groups we follow the procedure by Frisenda *et al.* [25]. Pure OPE3 is a powder, that we dissolve in dichloromethane at a concentration of 1 mmol/l. For splitting off the protecting acetyl groups we use a hydrate of tetrabutylammonium hydroxide (TBAH) solution of 10 mmol/l. The solutions were prepared by sonication for one hour to fully dissolve the compounds. Immediately following sonication of the solutions, the deprotection was done by adding 42 μL of the TBAH solution to 2 mL of the OPE3 solution. The color of the OPE3 solution changes from a pale yellow to a slightly brighter yellow.

The procedure for deposion of molecules on the junction proceeds according to the following steps. Under continuous flow of dry nitrogen the gold junction is broken by manual control and reformed to verify that the mechanism is working properly. A drop of the solution is then deposited, immediately after deprotection. The contact is then broken again to allow the OPE3 to completely cover the electrodes. The vacuum can is then closed, evacuated and the system is cooled down by immersion of the dip-stick sample holder into liquid helium.

3. Results

For reference we first show data for clean gold contacts at 4.2 K, without applying the OPE3 solution. The conductance is measured while the contact between the electrodes is repeatedly broken. The data from the digitized conductance curves obtained in this way are collected in a data set, sorted according to the conductance values, and plotted in the form of a histogram, as shown in Fig. 3. The inset shows a linearly-binned histogram for all conductance values observed in the range from 0 to 5 G_0, using gain settings of the current amplifier of 10^5 V/A. It reproduces the familiar peaks for gold associated wtih the discrete atomic structure of the contact, in combination with a limited set of conductance channels. The very characteristic strong peak near 1 G_0 reflects the sharply defined conductance of Au atomic contacts and one-dimensional atomic chains.

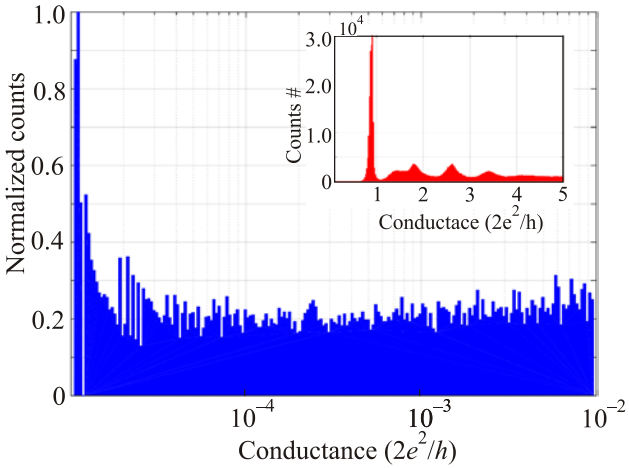

Fig. 3. (Color online) Logarithmic conductance histogram for a clean gold junction for low conductance, obtained from about 800 breaking traces at 4.2 K. The inset shows a linearly-binned histogram in the high-conductance regime obtained from about 4500 traces.

The information on single molecules bridging the junction is expected to be found in the low-conductance regime, in the low-end tail of the distribution shown in the inset. In order to bring out the features connected to such molecular junctions we increase the amplifier setting to 10^8 V/A, and we use logarithmic binning of the conductance values into a histogram. Some authors use a logarithmic current amplifier, which has the advantage that many decades in conductance can be covered at once. For the present setting of our linear current amplifier we are limited at the low end at $10^{-5}G_0$ by the noise floor of the amplifier, and at the high end at $10^{-2}G_0$ by the saturation of the amplifier. We have verified by using other amplifier settings that the relevant information for OPE3 is contained within our conductance window. A logatithmic histogram for clean gold obtained with these settings is shown in the main pannel of Fig. 3 for reference. It shows a flat featureless background signal, expected for a cleanly breaking contact. The rise at the low end of the range is attributed to tunnel current contributions and to the noise of the amplifier. The counts in the histogram have been normalized to the highest peak in the spectrum.

After deposition of OPE3 the histogram in the low-conductance regime changes markedly. Already at room temperature a broad asymmetric peak becomes visible at about $2\cdot10^{-4}G_0$ (not shown here), in agreement with the typical conductance values for OPE3 reported in the literature [24,25,27,28]. Approximately 10% of the recorded traces contained signatures of OPE3 here. While this already demonstrates that the NW-MCBJ technique can be employed for the investigation of thiol-coupled molecules, the most remarkable observation was made when cooling

down to liquid helium temperatures. After reaching helium temperatures it required several attempts at deep indentation of the wire ends for signatures of OPE3 molecules to manifest themselves in the conductance traces. But as soon as they appeared they persisted in a large number of subsequent traces. Figure 4(a) shows a logarithmic histogram for 900 breaking traces. The histogram has a sharp peak at $1.3 \cdot 10^{-4} G_0$, and has an unprecedently narrow width of only 40% at FWHM. The typical width of the conductance histogram for such molecular junctions is one decade.

We gain more insight into the nature of the sharp conductance peak by making a rupture trace density plot. The same data as for the histogram we re-analyzed by aligning the points of metal-metal contact breaking in the horizontal axis for all curves. In practice we identify this point as the point with the steepest slope, and it occurs when the conductance suddenly drops below the gold atomic contact value of 1 G_0. Figure 4(b) shows a color coded plot of the density of points obtained in the plane spanned by displacement (x-axis) and conductance (y-axis). The conclusion we draw from this graph is that the far majority of breaking traces follows the same pattern. The finite width of the peak in the conductance histogram is not the result of statistical variation in the molecular junction properties, but is an intrinsic property of the dependence of the molecular junction on the state of stretching of the junction. The reproducibility of the conductance traces exists despite the fact that the range of displacement is about 8 nm, much larger than the size of the molecule of less than 2 nm. During the breaking cycles the indentation of the metal-metal contacts is at least 3 nm, equivalent to a conductance of several times the conductance quantum. It seems plausible that a single OPE3 molecule is being repeatedly caught in the same junction configuration.

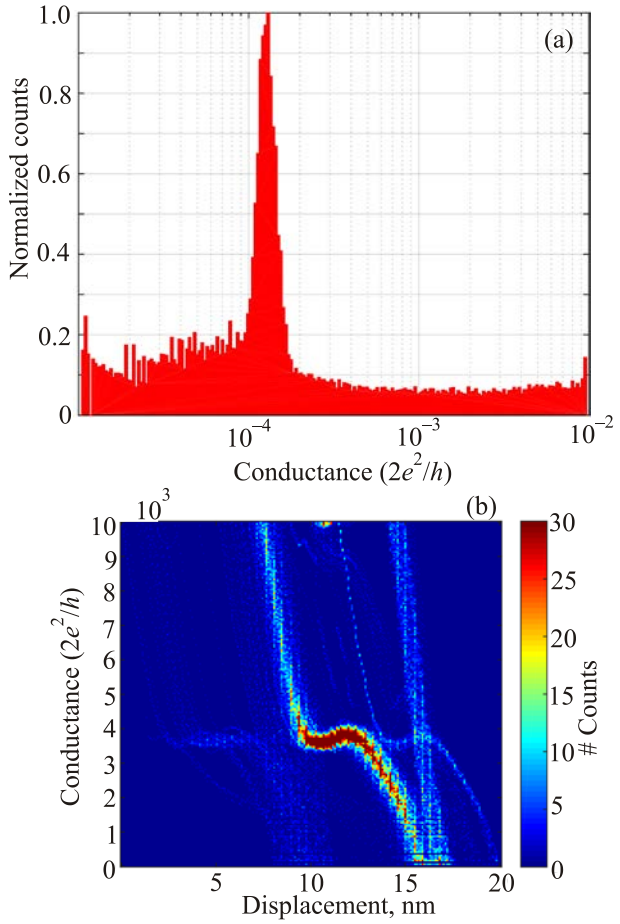

Fig. 4. (Color online) Conductance histograms for OPE3 molecular junctions at 4.2 K. (a) Logarithmic one-dimensional conductance histogram showing the counts of conductance data collected for the first 900 breaking cycles of the NW-MCBJ junction. (b) The same data represented as a two-dimensional color coded histogram, with the electrode displacement plotted along the horizontal axis.

The data shown in Fig. 4 represent the first 900 breaking cycles. Continuing the measurements beyond this point and taking into account the full set of rupture traces yields a much broader peak in the conductance histogram, as shown in Fig. 5. This peak has an appearance and a width that is much better comparable with typical results presented in the literature [24,25,27]. However, in our case the wide peak appears as if being a superposition of several sharper peaks with slightly shifted conductances. This is confirmed by splitting the data set into three subsets of consecutively recorded traces, as depicted in Fig. 5. This observation suggests that at least three different contact configurations have been probed. Each of the three is highly reproducible, but spontaneous switches from one configuration to the next occur that make the previous configuration inaccessible.

The single-molecule OPE3 junctions in the NW-MCBJ are surprisingly stable. When holding the voltage applied to the piezo actuator steady at a conductance plateau be-

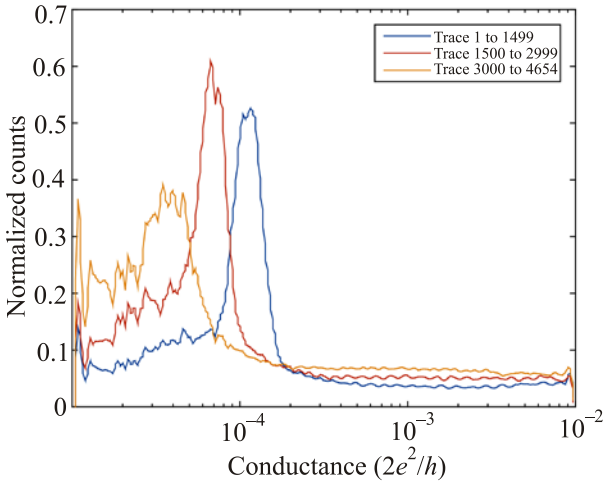

Fig. 5. Logarithmic conductance histogram of OPE3 at 4.2 K built from 4654 rupture traces, including the first 900 of Fig. 4. The histogram shows a broad peak which can be decomposed into several distinct peaks indicating different configurations of OPE3 anchoring to the gold electrodes.

longing to a OPE3 molecule the conductance was held stable for more than two hours. In order to test for sensitivity of the junction towards external vibrations we on purpose induced vibrations to the cryostat. The setup had to be shaken heavily before the contact eventually broke. The molecular bridge also survives bias voltage excursions of 400 mV, but repreated pulses of 1 V removed the molecules from the contact area. Long sequences of 1 V pulses (20 minutes) appear to result in permanently expelling all molecules from the junction area. After this we obtain conductance histograms characteristic of clean gold again.

4. Conclusions

We have demonstrated that NW-MCBJ can be used for the study of thiol-coupled molecules, and that conductance histograms can be obtained by rapid contact breaking cycles under piezo-electic control. Further, a method for deposition of dithiol coupled molecules to Au electrodes has been developed and tested succesfully.

As a first remarkable observation we find exceptionally sharp conductance histogram peaks for about 1000 conductance breaking cycles. We attribute the sharp peaks to precisely recurring molecular configurations. At the same time we find that the regularly found broad histogram peaks reported in the literature can be attributed to inhomogenous broadening resulting from the contribution of many different molecular configurations. The reproducibility of molecular configurations is possibly related to a similar phenomenon observed for atomic contacts [29]. After training metallic contacts, i.e. applying many cycles of contact making and breaking, the conductance is found to repeatedly retrace the same evolution during breaking. This has been attributed to the effect of mechanical annealing, which removes defects from the junction area and induces ordered stacking of the atoms near the contact. We speculate that for such annealed contacts a molecule present in the junction may also retrace the same conductance many times. The fact that this has not been reported before may be associated with the fact that L-MCBJ are usually opperated by mechanical motor control, which is much less precisely repeatable than the piezo control, allowed for NW-MCBJ [15].

The observations indicate that only a single molecule takes part in the process. Although the method of deposition leads to a high degree of coverage of molecules over the metal surface, we suspect that hard closing of the junction during cool down expells a large part of the molecules. This explains why several deep-indentation attempts are required for molecular signatures to re-appear at low temperatures.

The molecular junctions are exceptionally stable. This stability may be explained by the observed reproducibility. When external mechanical perturbations induce a sudden change in the electrode distance, the junction recovers its initial configuration once this perturbation dies away. Such highly stable molecular junctions are very favorable for extended study of molecular junctions, as is needed when charactrizing the molecular bridge in detail by measuring inelastic excitation spectra and shot noise characteristics of the molecular junction.

This work was supported by the Netherlands Organisation for Scientific Research (NWO/OCW), as part of the Frontiers of Nanoscience program and is part of the research programme of the Foundation for Fundamental Research on Matter (FOM), which is financially supported by NWO. We thank Herre van der Zant for support and discussions.

1. C.J. Muller, J.M. van Ruitenbeek, and L.J. de Jongh, *Phys. Rev. Lett.* **69**, 140 (1992).
2. J.M. van Ruitenbeek, A. Alvarez, I. Piñeyro, C. Grahmann, P. Joyez, M. H. Devoret, D. Esteve, and C. Urbina, *Rev. Sci. Instrum.* **67**, 108 (1996).
3. H.B. Weber, J. Reichert, F. Weigend, R. Ochs, D. Beckmann, M. Mayor, R. Ahlrichs, and H. v. Löhneysen, *Chem. Phys.* **281**, 113 (2002).
4. N. Agraït, J.G. Rodrigo, and S. Vieira, *Phys. Rev. B* **47**, 12345 (1993).
5. B. Xu and N.J. Tao, *Science* **301**, 1221 (2003).
6. Y.S. Park, A.C. Whalley, M. Kamenetska, M.L. Steigerwald, M.S. Hybertsen, C. Nuckolls, and L. Venkataraman, *J. Am. Chem. Soc.* **129**, 15768 (2007).
7. R. Temirov, A. Lassise, F. Anders, and F. Tautz, *Nanotechnology* **19**, 065401 (2008).
8. G. Schull, Y. Dappe, C. González, H. Bulou, and R. Berndt, *Nano Lett.* **11**, 3142 (2011).
9. G. Reecht, C. Lotze, D. Sysoiev, T. Huhn, and K. Franke, *ACS Nano* **10**, 10555 (2016).
10. T. Miyamachi, M. Gruber, V. Davesne, M. Bowen, S. Boukari, L. Joly, F. Scheurer, G. Rogez, T. Yamada, P. Ohresser, E. Beaurepaire, and W. Wulfhekel, *Nature Commun.* **3**, 938 (2012).
11. D.J. Wold and C.D. Frisbie, *J. Am. Chem. Soc.* **123**, 5549 (2001).
12. N. Fournier, C. Wagner, C. Weiss, R. Temirov, and F.S. Tautz, *Phys. Rev. B* **84**, 035435 (2011).
13. H. Park, J. Park, A.K.L. Kim, P.L.M.E.H. Anderson, and A.P. Alivisatos, *Nature* **407**, 57 (2000).
14. E. Osorio, K. O'Neill, M. Wegewijs, N. Stuhr-Hansen, J. Paaske, T. Bjørnholm, and H. van der Zant, *Nano Lett.* **7**, 3336 (2007).
15. C.A. Martin, D. Ding, H.S.J. van der Zant, and J.M. van Ruitenbeek, *New J. Phys.* **10**, 065008 (2008).
16. N. Agraït, A. Levy Yeyati, and J.M. van Ruitenbeek, *Phys. Rep.* **377**, 81 (2003).
17. R.H.M. Smit, Y. Noat, C. Untiedt, N.D. Lang, M.C. van Hemert, and J.M. van Ruitenbeek, *Nature* **419**, 906 (2002).
18. S. Kaneko, C. Motta, G.P. Brivio, and M. Kiguchi, *Nanotechnology* **24**, 315201 (2013).

19. T. Yelin, R. Vardimon, N. Kuritz, R. Korytár, A. Bagrets, F. Evers, L. Kronik, and O. Tal, *Nano Lett.* **13**, 1956 (2013).
20. T. Yelin, R. Korytár, N. Sukenik, R. Vardimon, B. Kumar, C. Nuckolls, F. Evers, and O. Tal, *Nature Mater.* **15**, 444 (2016).
21. D. Rakhmilevitch, R. Korytár, R. Korytr, A. Bagrets, F. Evers, and O. Tal, *Phys. Rev. Lett.* **113**, 236603 (2014).
22. J. Reichert, R. Ochs, D. Beckmann, H.B. Weber, M. Mayor, and H. von Löhneysen, *Phys. Rev. Lett.* **88**, 176804 (2002).
23. D. Dulić, S.J. van der Molen, T. Kudernac, H.T. Jonkman, J.J.D. de Jong, T.N. Bowden, J. van Esch, B.L. Feringa, and B.J. van Wees, *Phys. Rev. Lett.* **91**, 207402 (2003).
24. R. Frisenda and H. van der Zant, *Phys. Rev. Lett.* **117**, 126804 (2016).
25. R. Frisenda, M.L. Perrin, H. Valkenier, J.C. Hummelen, and H.S.J. van der Zant, *Phys. Status Solidi B* **250**, 2431 (2013).
26. V. Kaliginedi, P. Moreno-García, H. Valkenier, W. Hong, V.M. García-Suárez, P. Buiter, J.L.H. Otten, J.C. Hummelen, C.J. Lambert, and T. Wandlowski, *J. Am. Chem. Soc.* **134**, 5262 (2012).
27. S. Wu, M. González, R. Huber, S. Grunder, M. Mayor, C. Schönenberger, and M. Calame, *Nature Nanotechnology* **3**, 569 (2008).
28. R. Huber, M.T. González, S. Wu, M. Langer, S. Grunder, V. Horhoiu, M. Mayor, M.R. Bryce, C. Wang, R. Jitchati, C. Schonenberger, and M. Calame, *J. Am. Chem. Soc.* **130**, 1080 (2008).
29. C. Sabater, C. Untiedt, J.J. Palacios, and M.J. Caturla, *Phys. Rev. Lett.* **108**, 205502 (2012).